Invited Paper

Quasi-phasematched optical parametric oscillators using bulk periodically poled $LiNbO_3$

L. E. Myers, R. C. Eckardt, M. M. Fejer, and R. L. Byer

E. L. Ginzton Laboratory, Stanford University, Stanford, California 94305

ABSTRACT

We review progress of quasi-phasematched (QPM) optical parametric oscillators (OPO's) in bulk periodically poled $LiNbO_3$. Using the electric field poling process, we can reliably fabricate 0.5-mm thick crystals with uniform domain structures over 15-mm long. Periodically poled material retains the low loss and bulk power handling properties of single domain $LiNbO_3$, and QPM allows noncritical phasematching with the highest value of the nonlinear coefficient. OPO's pumped by 1.064-μm pulsed Nd:YAG lasers have been operated over the wavelength range 1.45 μm to 4.0 μm with tuning by temperature or QPM period. We have shown oscillation threshold as low as 0.020 mJ with a Q-switched pump laser, and pumping over ten times threshold without damage. We have also demonstrated a doubly resonant oscillator near 1.96 μm pumped directly with a cw diode laser at 978 nm.

Keywords: quasi-phasematching, optical parametric oscillators, infrared sources, difference frequency generation

1. INTRODUCTION

Optical parametric oscillators (OPO's) are attractive sources of coherent radiation for applications where laser sources are unavailable or where wide tunability is needed. Recent interest in OPO's has been spurred by advances in stable pump lasers and improvements in nonlinear optical materials. Still, many desirable OPO implementations are limited by problems with conventional birefringent phasematching techniques in available materials, such as Poynting vector walkoff, low effective nonlinear coefficient, inconvenient phasematching temperature, and narrow acceptance bandwidths.

Quasi-phasematching (QPM) is an alternative technique to birefringent phasematching for compensating phase velocity dispersion in frequency conversion applications.[1] In a QPM device, the nonlinear coefficient is modulated with a period twice the coherence length of the interaction to offset the accumulated phase mismatch. A significant advantage of QPM is that any interaction within the transparency range of the material can be noncritically phasematched at a specific temperature, even interactions for which no birefringent phasematching condition can be found. Another benefit is that the interacting waves can be chosen so that coupling occurs through the largest element of the $\chi^{(2)}$ tensor. In $LiNbO_3$, QPM with all waves polarized parallel to the z-axis yields a gain enhancement over the birefringently phasematched process of $(2d_{33}/\pi d_{31})^2 \approx 20$.

Since the pool of mature materials is limited and the development cycle for new materials is long and costly, QPM is a useful technique for extending the operating range of available nonlinear optical materials. Using planar processing methods from the microelectronics industry, in particular lithography, practical microstructured materials for QPM interactions can be fabricated inexpensively. The ability to pattern QPM structures allows engineering the performance of the material for the desired interaction. The most straightforward application of QPM is in a device with a periodically modulated nonlinear coefficient, in which the grating vector of the periodic modulation pattern shifts the peak phasematching condition to the desired operating point. Engineering more complex behavior, such as broad band phasematching or multi-wavelength gratings, in principal involves nothing other than designing a more sophisticated lithographic mask.

2. FABRICATION OF PERIODICALLY POLED $LINBO_3$

Implementation of QPM requires a fabrication method that can achieve uniform micron-scale periodic structures while preserving the material's transparency, nonlinearity, and power handling capability. QPM was proposed before birefringent phasematching,[2] but difficulties in fabricating QPM materials have prevented its widespread use. Recent advances in fabricating practical QPM materials have renewed interest in this approach. $LiNbO_3$ has attracted special attention because it is a mature, readily available material with transparency covering a useful range from 0.35 μm to >4 μm. QPM can be

0-8194-1726-2/95/$6.00

implemented in a ferroelectric material such as $LiNbO_3$ by periodic reversal of the ferroelectric domains, since antiparallel domains correspond to a sign reversal of the nonlinear coefficient. Several techniques have been developed for producing periodically poled $LiNbO_3$ (PPLN). Chemical indiffusion has been used to make periodic structures of good quality; however, the pattern is limited to shallow layers which are sufficient for waveguide devices but lack the power handling capability required for many applications.[3,4] Bulk PPLN has been made by modulating the crystal growth process, but it suffers from axial variations in domain periodicity that significantly degrade efficiency.[5,6] Electron beam writing can produce bulk PPLN with good periodicity, but uniformity is poor and the process does not lend itself to manufacturability.[7] Recently, techniques for ferroelectric domain reversal with an external electric field have produced PPLN and periodically poled $LiTaO_3$ for QPM second harmonic generation.[8,9,10] In this approach, domain periodicity is precisely defined by a lithographic mask using standard micro-fabrication techniques. We have developed an electric field poling process that yields uniform PPLN in thick substrates for efficient QPM frequency conversion applications.[11]

We use standard optical-grade $LiNbO_3$ wafers of congruent composition with the configurations shown in Figure 1. The positive electrode is patterned on the $+z$ surface with the desired structure. We have used two variants for this electrode fabrication. In the first approach, a 0.2-μm-thick aluminum grating is patterned using lift-off lithography. A 2-μm-thick layer of photoresist is applied over the grating leaving a portion of the metal pattern exposed. Contact is made to the exposed metal with a liquid electrolyte consisting of LiCl in deionized water. In the second variation, a grating pattern of photoresist is covered by a 0.2-μm thick aluminum film, and then covered by the electrolyte. In both cases, the photoresist layer insulates the electrode lines, inhibits domain growth between the grating lines, and forms the contour of an isopotential surface when covered with the electrolyte. The isopotential surface controls fringing fields at the edges of the grating lines, improving pattern uniformity and resolution. The first method (insulator over conductor) seems to produce better pattern fidelity, probably because the well-defined edges of the metal lines produce a more homogeneous field condition than the tapered photoresist edges in the second method. The second method (conductor over insulator) is easier to fabricate with a single lithography step, and it provides pattern quality sufficient for the feature sizes of IR devices. We have also patterned

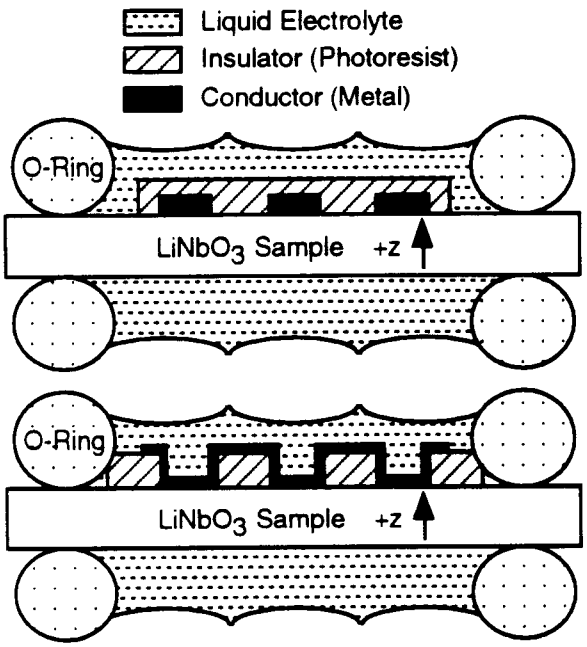

Fig. 1. Electrode configurations for electric field poling. The upper figure shows a variation with insulator over conductor; the lower figure shows conductor over insulator. In both cases, the covering electrolyte forms an isopotential surface that helps control fringing fields around the pattern.

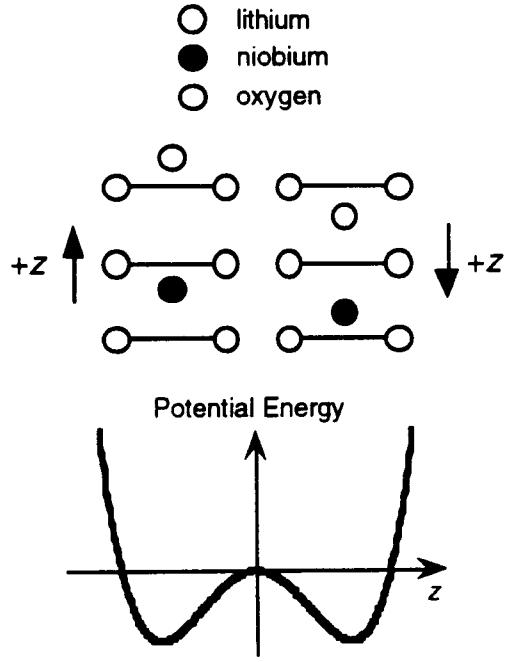

Fig. 2. Qualitative picture of ferroelectricity in $LiNbO_3$. Domain polarity is determined by the direction of offset of the metal ions relative the oxygen lattice. Domains can be reversed by application of a field sufficient to overcome the energy barrier.

the $+z$ surface directly with photoresist trenches and liquid contact,[12] but we found that the metal/$LiNbO_3$ contact enhanced the poling in that region. For the negative electrode, liquid electrolyte is applied directly to the bare $-z$ surface. The liquid electrode fixture consists of two electrolyte-containing chambers which squeeze the $LiNbO_3$ sample between o-rings. This arrangement allows application of fields exceeding 25 kV/mm without breakdown of the sample and without the need for surrounding oil or vacuum. The choices of aluminum for the metal, photoresist for the insulator, and LiCl solution for the liquid contact are convenient but not necessarily optimal, making this an area for future research efforts.

A qualitative picture of ferroelectricity in $LiNbO_3$ is shown in Fig. 2. Polarity of a ferroelectric domain is determined by the offset of the metal ions either above or below the oxygen lattice.[13] Domain reversal involves reorienting the crystal from one stable configuration to the other, which can be effected by the application of an external electric field. Significant domain reversal occurs when the applied field exceeds a certain level referred to as the coercive field, which is ~21 kV/mm for $LiNbO_3$ at room temperature. Domain reversal is permanent after roughly 50 ms. When the voltage is abruptly turned off, domains that flipped in the last ~50 ms will flip back to their original orientation. For slow poling, such as we typically use, this flip back is negligible. However when the poling rate is fast, the material that flips back may represent a sizable portion of the domain-reversed region. Continuing to apply voltage for instance at a level half of the coercive field value, ramping the voltage off gradually on the time scale of 50 ms, and blocking back flow of charge with a series diode are effective means of preventing flip back of domains.

The poling circuit consists of a high voltage source with a series resistor R_s to regulate the current, as shown in Fig. 3. Typical scope traces of voltage and current measured during poling are shown in Fig. 4. With no sample in the circuit, the high voltage supply V_1 is set to produce the desired voltage pulse at V_2 so the field on the sample exceeds the coercive field. When the sample is added to the circuit and the same voltage pulse is applied, current flows through the circuit as the domain polarity reverses. The voltage on the sample clamps at the coercive field value, as explained by the following rationale. The poling current lowers the voltage across the sample by the voltage drop in the series resistor. As the voltage decreases below the coercive field level, poling slows down causing less voltage drop in the resistor. As less voltage drops in the resistor, the voltage on the sample increases above the coercive field level and more poling current flows, again increasing the voltage drop in the series resistor. Thus the voltage on the sample clamps at the coercive field level, and the series resistor regulates the current flow in the circuit.

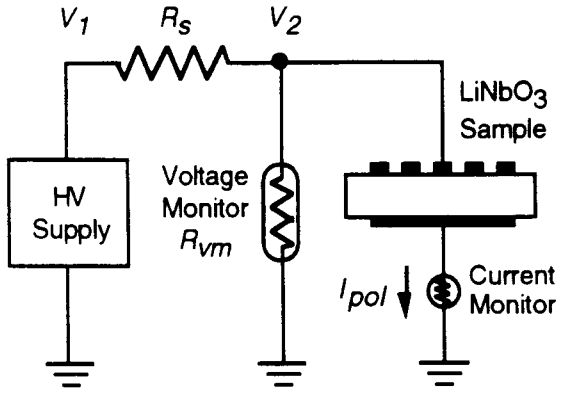

Fig 3. Electric field poling circuit. Typically R_s = 100 MΩ, R_{vm} = 1 GΩ, and V_2 is set at 12 kV for a 0.5-mm thick $LiNbO_3$ sample. During poling, V_2 clamps at the coercive voltage V_c.

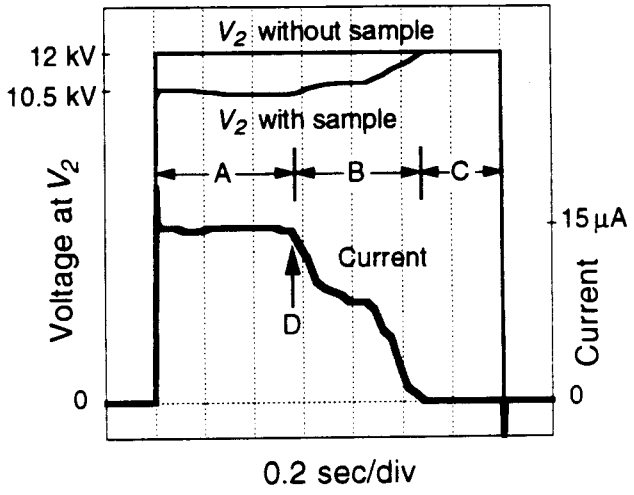

Fig. 4. Voltage and current waveforms for poling a 3-mm diameter, 0.5-mm thick piece of $LiNbO_3$. Section A is poling under the metal or liquid contact. Section B is poling under the photoresist. Section C is after completion of poling. For a patterned device, the voltage would be turned off at point D.

The poling current I_{pol} is given by:

$$I_{pol} = \frac{V_1 - V_c}{R_s} - \frac{V_c}{R_{vm}}$$

where V_1 is the supply voltage before the series resistor R_s, V_c is the voltage corresponding to the coercive field level, (~21 kV/mm) and R_{vm} is the impedance of the voltage monitor. Current of 13 μA to 33 μA was used to pole the devices reported in this paper. By varying the driving voltage V_1 and the series resistance R_s, we have performed testing at currents up to 10 mA, but the lower current tended to produce straighter domain walls. The duration of the poling current depends linearly on the area being poled. The charge Q transferred to the sample is that required to compensate the reversed orientation of the spontaneous polarization, given by $Q = 2P_S A$ where P_S is the spontaneous polarization of $LiNbO_3$, A is the area of the domain-reversed region, and the factor of 2 accounts for the polarity reversal. A published value of P_S is 0.71 C/cm^2,[14] but we have found that a value 10% higher gives better agreement in our work. The duration of poling is the time needed for the charge transfer during domain reversal.

Patterning is accomplished by controlling the charge transfer that accompanies domain reversal. Domain growth is almost instantaneous in the z-direction, so the poling current represents primarily lateral domain growth in the x- and y-directions. The conductivity of $LiNbO_3$ is low enough that the poling current can readily be monitored. The scope trace in Fig. 4 is the poling current and voltage for a 3-mm diameter sample with a patterned electrode on the $+z$ surface. The initial plateaus (section A) in the current and voltage indicate poling taking place under either liquid or metal in direct contact with the $LiNbO_3$. The middle region (section B) with lower current indicates poling under the photoresist at a higher coercive voltage. The end of the pulse (section C) where no current flows indicates completion of domain reversal. The strategy for domain patterning is to stop the voltage pulse before the poling progresses under the photoresist (point D). We typically do this by limiting the pulse duration at a given current and driving voltage level while monitoring the current and charge transfer. Another approach is to lower the applied field below the coercive field of the photoresist-covered material. The series impedance can be adjusted or eliminated to achieve the desired poling rate. Computer control is useful in monitoring poling and determining a stopping criterion.[10]

The domains typically grow beyond the line width defined by the grating lithography due

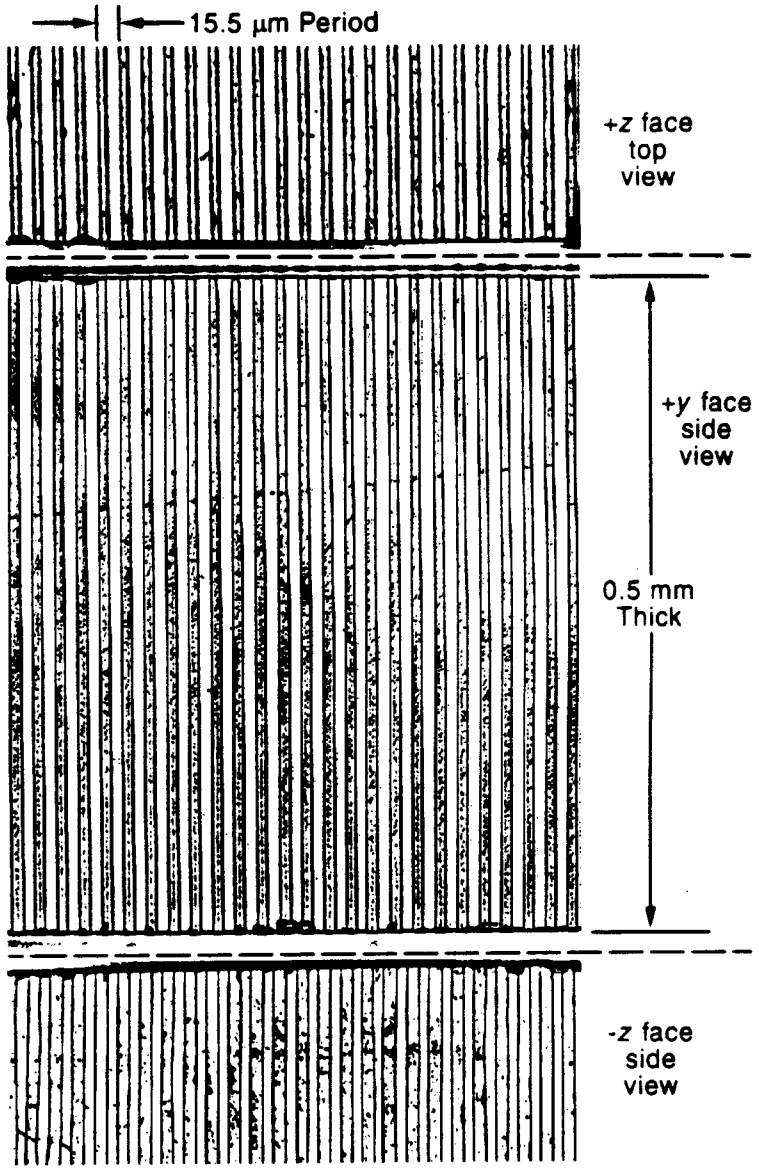

Fig. 5. Orthographic view of 0.5-mm thick PPLN with a 15.5-μm period, after etching in HF acid to reveal the domain structure. The three panels are top, side, and bottom views taken at the same location in the crystal by cutting and polishing into the grating region. The top panel is the $+z$ face on which the lithographic electrode was applied. The middle panel is a cross sectional view of the $+y$ face. The bottom panel is the $-z$ face which had the unpatterned ground electrode.

to remaining fringing fields at the line edges. For devices with periods of interest for infrared applications (i.e. periods > 10 μm), a rule of thumb is that the domain width will be ~3-4 μm wider than the pattern line width. The electrode structures described above are effective in making this domain width uniform over the poled region. The lithography pattern can be adjusted to take into account this resultant domain size. Shown in Fig. 5 is a cross sectional view of a PPLN sample, illustrating the straight, vertical domain boundary walls throughout the material volume. We currently make 0.5-mm thick device-quality PPLN with 15-mm long poled regions. In the future, we expect to be able to make PPLN 1-mm thick and 5-cm long.

3. PPLN DIFFERENCE FREQUENCY GENERATION EXPERIMENTS

To verify domain pattern homogeneity for infrared parametric interactions, we performed a difference frequency generation (DFG) experiment using a sample with 15.5-μm grating period similar to that shown in Fig. 5. The end faces of the crystal were polished down to the periodically poled region such that the finished device was 2.2-mm long. Pump radiation from a cw Ti:sapphire laser tunable near 710 nm and signal radiation from a 1.555-μm cw erbium fiber laser were mixed in the PPLN crystal. The single-pass idler power generated near 1.3 μm is shown in Fig. 6, along with the theoretical tuning curve. The ripples in the measured data are due to interference effects of Fresnel reflections from the uncoated polished end faces of the crystal. The bandwidth of the theoretical curve is as calculated from the Sellmeier coefficients for bulk $LiNbO_3$ at room temperature;[15] the phasematching peak has been shifted +1 nm by a change in the dispersion of $\sim 10^{-4}$ which is within the accuracy claimed for the Sellmeier fit. The significance of this result is that the tuning curve shows a single well-defined peak with near theoretical bandwidth, demonstrating coherent interaction over the length of the sample.

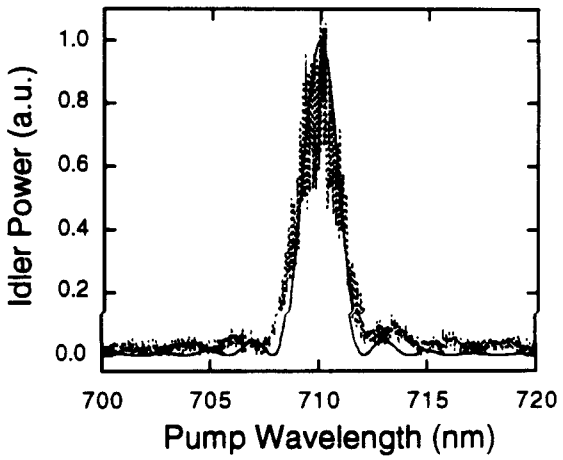

Fig. 6. DFG tuning curve for 15.5-μm period, 2.2-mm long PPLN, with λ_s = 1.555 μm and $\lambda_i \approx$ 1.3 μm. The calculated curve (solid line) is based on the Sellmeier coefficients at 25 °C with peak shifted +1 nm to match the data.[15] The fringes in the data are due to Fresnel reflections from the uncoated end faces.

DFG is itself a useful means of making a tunable source for some applications. In collaboration with SDL, we demonstrated generation of 3.6-4.0 μm radiation by difference frequency mixing of high power tunable laser diodes in bulk PPLN.[16] Up to 6 μW of output was obtained with a conversion efficiency comparable to that of $AgGaS_2$, which can also be noncritically phasematched under certain conditions. The advantage of PPLN is that QPM allows the freedom to select pump or signal wavelengths independent of phasematching requirements so that common diode laser sources can be used. In our demonstration, the 21-μm PPLN period allowed mixing diode lasers with convenient wavelengths around 980 nm and 777 nm to obtain the desired mid-IR output.

4. PPLN OPO EXPERIMENTS

4.1. PPLN OPO's pumped by Q-switched Nd:YAG lasers

Pumping with Q-switched lasers offers an effective way of generating high gain in a simple cavity configuration which proved useful in our initial OPO demonstrations with the short interaction lengths of PPLN available at that time. With a 5-mm long PPLN crystal having 31-μm period, we demonstrated the first quasi-phasematched OPO in a bulk nonlinear optical

material.[11] As shown in Fig. 7, this singly resonant OPO produced output continuously tunable from 1.66 to 2.95 μm with heating from room temperature to 180 °C. The key results of this experiment were that no excess loss in the PPLN material was observed, and the damage limit was unchanged from its value for single domain $LiNbO_3$ of 3 J/cm^2 in a 10 ns pulse.[17] The measured threshold was near the theoretical value predicted by a pulsed singly resonant oscillator model.[17] A factor of ten margin between oscillation threshold and damage limit observed in our experiment indicates the potential utility for PPLN OPO's of this type.

Since the initial demonstration, we have operated PPLN OPO's with longer interaction lengths, different domain periods, and pumped by high repetition rate Q-switched Nd:YAG lasers in collaboration with Lightwave Electronics Corp. We have obtained singly resonant thresholds as low as 0.020 mJ and oscillation at up to 40 kHz pulse repetition rate with 15-mm long pieces. With a 28.5-μm period piece and a Nd:YAG pump laser operating at 1 kHz, we achieved idler output of 5 mW_{av} at 4 μm.[18]

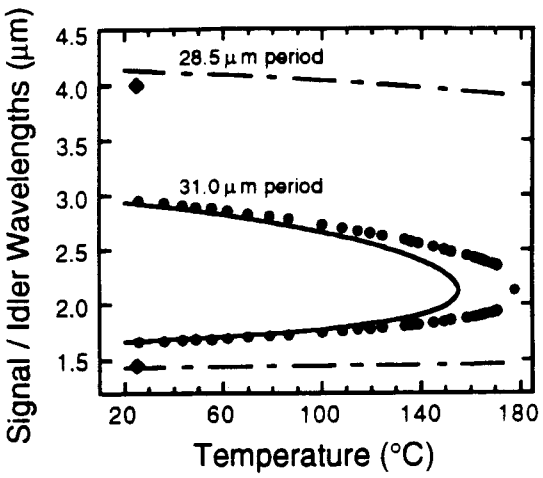

Fig. 7. Temperature tuning curves for 1.064-μm-pumped OPO in bulk PPLN with 31-μm and 28.5-μm periods. The calculated curves are based on the Sellmeier coefficients and include thermal expansion.[15,19] The offset between the data and theory is within the accuracy of the Sellmeier fit.

4.2. Long Pulse PPLN OPO's

In collaboration with Lightwave Electronics Corp., we have operated an OPO pumped by a 1.064-μm Nd:YAG laser with pulse duration of 0.1 - 1 μs.[20] The source was a 700-mW single-frequency cw Nd:YAG laser which was acousto-optically chopped and amplified in a multi-pass Nd:YAG amplifier. The resulting pump pulse had the temporal profile of a decaying exponential riding on a dc level, with initial peak power up to 300 W. For a PPLN crystal with 31-μm period and 15-mm length, the OPO threshold was 60 W peak and its pulse duration could be varied from 150-600 ns. By observing the long flat tail of the transmitted pump pulse, the steady state pump depletion level was measured to be 26 W. Since the cavity was not resonant at the idler (<1.5% feedback) and the OPO could be pumped over three times above threshold, it behaved like a singly resonant oscillator.[21] Therefore the saturated pump depletion level of 26 W provides a measurement of cw SRO threshold, which agrees with the predicted value.[22] This pump level is within the reach of current single-frequency cw Nd:YAG lasers, offering the potential for a useful high power mid-infrared source.

4.3. CW PPLN OPO's

For doubly resonant oscillators (DRO's) in PPLN, calculations predict thresholds readily within range of commercially available pump sources. An OPO directly pumped by a diode laser is especially interesting as a compact and efficient source of tunable radiation. Previous attempts using available nonlinear optical materials have been hampered because the gain and phasematching conditions placed difficult constraints on the wavelength and power requirements of the pump laser.[23] With the engineerable phasematching and high gain properties available through quasi-phasematching, we recently demonstrated the first OPO directly pumped by a commercial cw diode laser.[24]

The PPLN crystal for the diode-pumped OPO was 0.5-mm thick with a 9.3-mm interaction length. The domain period for quasi-phasematching was 28.5 μm, designed for degenerate operation at 88°C as shown in Fig. 8.[15] The experiment, performed in collaboration with Cygnus Laser Corp., used a 977.6-nm master oscillator/power amplifier (MOPA) diode laser from SDL, Inc (model 5762). We operated the laser at 500 mW and used a scanning confocal interferometer with a resolution of 25 MHz to verify single frequency operation.

The doubly resonant OPO resonator was a linear cavity with 10-mm radius of curvature mirrors separated by 22 mm. The output coupler was mounted on an annular piezoelectric element for cavity length control. The OPO output near 1.96 μm was detected with a PbS detector after a filter that blocked the pump beam; while the transmitted pump beam was detected with a Si detector. Fig. 9 shows the cavity mirror piezo voltage, pump transmission through the cavity, and the OPO output through a 0.7% output coupler as the cavity length was scanned with the piezo. The threshold was 61 mW and 98 mW for 0.3% and 0.7% output couplers respectively, which agree with calculated values for a DRO.[22] The peak phasematching temperature was measured at 91°C which agrees with the design calculation shown in Fig 8. For 370 mW of pump incident on the cavity mirror, we measured peak output powers of 34 mW and 64 mW for 0.3% and 0.7% output couplers respectively. The conversion efficiencies of 9% and 17% agree with the values obtained from pump depletion and with a theoretical calculation for a DRO.[22] Note in Fig. 9 where the piezo position was held at a resonant point for the OPO during the flat part before the voltage ramp. The relatively stable nature of the output at this point indicates the potential for adding control electronics to make a useful cw infrared tunable source.

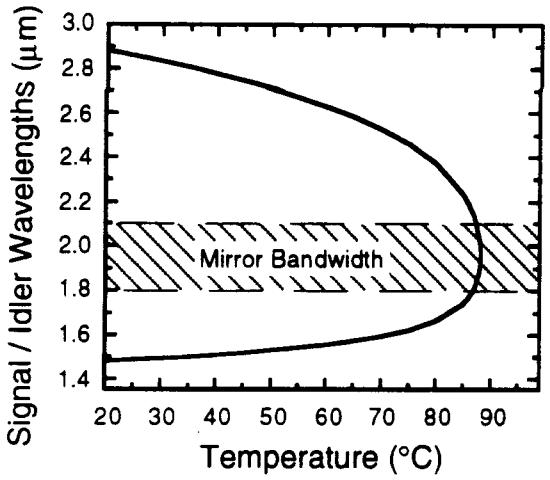

Fig. 8. Temperature tuning curve for 977.6-nm-pumped, 28.5-μm period PPLN OPO. Phasematching temperature at degeneracy is 88 °C. The bandwidth of the mirrors used in the diode-pumped OPO experiment is shown by the crosshatched region.

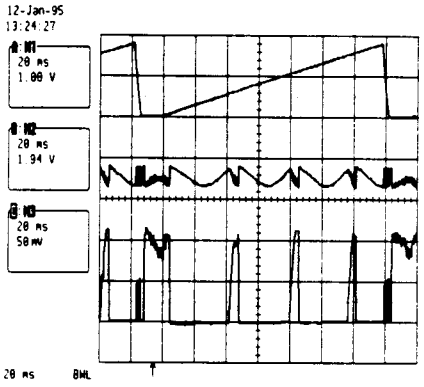

Fig. 9. Cavity mirror scan voltage, pump transmission with depletion, and ~1.96-μm OPO output signals.

5. FUTURE RESEARCH EFFORTS

The average power handling of $LiNbO_3$ is quite good. For example, a previous resonant second harmonic generation experiment in bulk PPLN fabricated by a fiber growth technique demonstrated power handling capability of 2 W cw at 0.532 μm and 65 W of circulating 1.064-μm cw power with a 15-μm waist.[25] With this power handling benchmark and the cw singly resonant oscillator threshold of ~26 W described in Section 4.2, high power PPLN OPO operation is feasible. However our attempts at high power cw pumping have been hindered by photorefractive damage. The damage is due to green light produced by non-phasematched, but enhanced, second harmonic generation. PPLN has previously been found to be resistant to photorefractive damage. Using bulk PPLN grown by the laser-heated pedestal technique, no photorefractive damage was observed with exposure to 100 mW at 0.488 μm.[26] With MgO-doped PPLN grown by the same technique, no photorefractive damage was observed in a resonant second harmonic generation experiment producing 300 mW of 0.532 μm light at room temperature and 1.7 W at 140 °C.[25] The mechanism for resistance to photorefractive damage in PPLN appears to be related to a cancellation effect in the oppositely-oriented domain regions. For IR devices with periods ~30 μm, this cancellation is less effective than in visible devices with periods <6 μm. Even a small amount of loss introduced by photorefractivity can be disastrous for cw OPO operation. Our plans to reduce photorefractive damage effects include heating the crystals, altering the domain structure to minimize green generation, and using periodically poled MgO:$LiNbO_3$.

QPM implemented with planar processing methods allows engineering the phasematching properties by design of the lithographic mask. More sophisticated QPM structures than the simple gratings used in the above experiments allow modification of the phasematching behavior.[1] Broad band phasematching and second harmonic generation with fanned gratings have been employed in PPLN waveguides.[27,28] We plan to make an electric-field-poled bulk PPLN chip with a fanned grating structure on it, so that the device will be tuned by scanning the chip transversely and allowing the beam to interact with different grating periods at different positions. The calculated tuning behavior as a function of grating period for a 1.064-μm pumped-OPO is shown in Figure 10. With suitable design, the entire mid-IR tuning range of $LiNbO_3$ can be accessed through simple translation of the crystal by <10 mm.

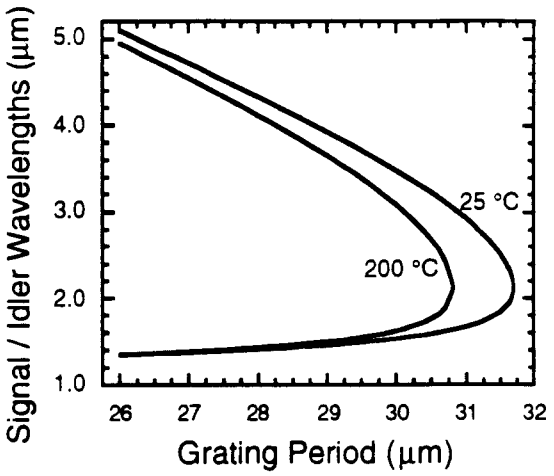

Fig. 10. Calculated tuning of 1.064-μm-pumped PPLN OPO with a fanned QPM grating period.[15]

6. CONCLUSION

Bulk PPLN is an exceptional material for OPO applications. PPLN fabricated with the electric field poling method retains the low loss and damage qualities of single domain $LiNbO_3$, while QPM allows noncritical phasematching with the highest value of the nonlinear coefficient giving a nonlinear drive larger by a factor of 20 than the comparable birefringently phasematched process. Electric field poling can reliably produce devices suitable for OPO and DFG interactions through the mid-IR transparency range of the material. Using PPLN, we have successfully demonstrated the first QPM OPO in a bulk nonlinear optical material, and the first OPO directly pumped by a commercial cw diode laser. PPLN promises to be an important material for future applications requiring sources in the range 1 μm to >4 μm.

ACKNOWLEDGMENTS

We thank G. D. Miller for collaboration during the development of the electric field poling process, M. L. Bortz for performing DFG measurements, and Crystal Technology, Inc. for supplying $LiNbO_3$ wafers. We acknowledge W. R. Bosenberg of Lightwave Electronics Corp., J. W. Pierce of Cygnus Laser Corp., and S. Sanders of SDL, Inc. for collaboration in performing the OPO and DFG experiments. This work was supported by the Office of Naval Research, the USAF Phillips Laboratory, and ARPA through the Center for Nonlinear Optical Materials at Stanford University. L. E. Myers acknowledges the support of the US Air Force.